

### Some N<sup>12</sup> and B<sup>12</sup> Beta-Decay Measurements\*†

R. W. PETERSON AND N. W. GLASS

Los Alamos Scientific Laboratory, University of California, Los Alamos, New Mexico

(Received 26 November 1962)

The branching fractions of the B<sup>12</sup> and N<sup>12</sup> beta decays to the 4.43-MeV level of C<sup>12</sup> were determined to be (1.3±0.1)% and (2.4±0.2)%, respectively, by means of βγ-coincidence measurements. The B<sup>12</sup> and N<sup>12</sup> half-lives were remeasured, using a beta-ray spectrometer to identify the emitted beta particles, and found to be 20.2±0.2 msec and 11.0±0.1 msec, respectively. The thin-target cross-section curve for the B<sup>10</sup>(He<sup>3</sup>,n)N<sup>12</sup> reaction was measured over the energy range from 2.0 to 6.3 MeV. Using the above half-lives and branching ratios, the ratio of the N<sup>12</sup> to B<sup>12</sup> ft values for transitions to the 4.43-MeV level of C<sup>12</sup> was calculated to be 0.92±0.06. With the use of published data and the above half-lives, the ratio of ft values of the N<sup>12</sup> to B<sup>12</sup> ground-state transitions was calculated to be 1.16±0.03. Thus, there appears to be a significant difference in the B<sup>12</sup> and N<sup>12</sup> ground-state transition ft values.

#### PART I

#### N<sup>12</sup> and B<sup>12</sup> Branching Ratios to the 4.43-MeV Level of C<sup>12</sup>

BY means of beta emission N<sup>12</sup> and B<sup>12</sup> decay to the ground state and excited levels of C<sup>12</sup>. The known decays are indicated by arrows on the brief C<sup>12</sup> energy-level diagram shown in Fig. 1. The branching fractions listed by Ajzenberg-Selove and Lauritsen<sup>1</sup> are shown on the B<sup>12</sup> decays. The numbers in parentheses on the N<sup>12</sup> transitions are the relative amounts of each transition, based on a value of 100 for the ground-state transition, as measured by Vedder.<sup>2</sup>

The branching ratio of B<sup>12</sup> to the 4.43-MeV level of C<sup>12</sup> has been measured by Kavanagh and Barnes<sup>3</sup> to be (1.4±0.4)%, by Tanner<sup>4</sup> as (1.7±0.4)%, and by Vedder<sup>2</sup> as (6±3)%. Ajzenberg-Selove and Lauritsen<sup>1</sup> give (1.5±0.3)% as the average of these values. Vedder<sup>2</sup> also measured the branching ratio of N<sup>12</sup> to the 4.43-MeV level of C<sup>12</sup> to be 15% of the ground-state transitions, with no quoted error. If charge symmetry is assumed, these values of the branching ratios of N<sup>12</sup> and B<sup>12</sup> to the 4.43-MeV level of C<sup>12</sup> are in considerable disagreement. Therefore, it was felt worthwhile to make a more precise measurement of these branching ratios, from which the ratio of ft values of transitions to the 4.43-MeV level of C<sup>12</sup> could be calculated, to determine whether or not a real inconsistency existed.

Also, more precise values of these same branching ratios were desirable for the experimental comparison of the shapes of the B<sup>12</sup> and N<sup>12</sup> ground-state spectra carried out subsequently.<sup>5,6</sup> With the branches to the

4.43-MeV level known, the shapes of the ground-state spectra can be determined from the measured N<sup>12</sup> and B<sup>12</sup> beta spectra from the end-point energies back to the energies where the contributions from the beta groups to the 7.66-MeV level of C<sup>12</sup> become appreciable.

The two desired activities were formed by means of the B<sup>10</sup>(He<sup>3</sup>,n)N<sup>12</sup> and B<sup>11</sup>(d,p)B<sup>12</sup> reactions. Thick targets of boron powder pressed into a disc shape onto a 5-mil brass backing were bombarded by 3-MeV He<sup>3</sup> particles and 2-MeV deuterons from the large Los Alamos Van de Graaff. Normal boron targets were used with deuteron bombardment, and boron targets enriched to 96% B<sup>10</sup> were used with the He<sup>3</sup> beam. The beam was gated by means of a square voltage pulse applied to an electrostatic deflector which was located

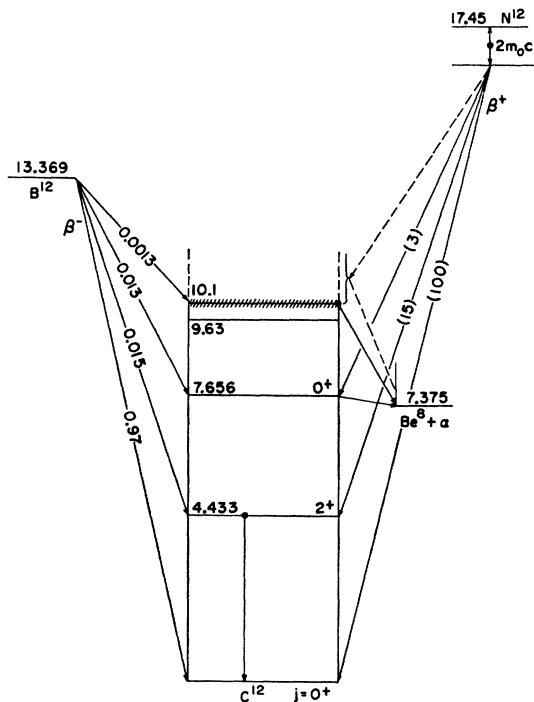


FIG. 1. Partial energy level diagram of C<sup>12</sup> showing the B<sup>12</sup> and N<sup>12</sup> decays to levels of C<sup>12</sup>.

\* Work performed under the auspices of the U. S. Atomic Energy Commission.

† A preliminary report of this work was given at the 1961 New York meeting of the American Physical Society [Bull. Am. Phys. Soc. 6, 49 (1961)].

<sup>1</sup> F. Ajzenberg-Selove and T. Lauritsen, Nucl. Phys., 11, 1 (1959).

<sup>2</sup> J. F. Vedder, University of California Radiation Laboratory Report UCRL 8324, 1958 (unpublished).

<sup>3</sup> R. W. Kavanagh and C. A. Barnes, Phys. Rev. 112, 503 (1958).

<sup>4</sup> N. Tanner, Phil. Mag. 1, 47 (1956).

<sup>5</sup> N. W. Glass and R. W. Peterson, following paper [Phys. Rev. 129, 299 (1963)].

<sup>6</sup> T. Mayer-Kuckuk and F. C. Michel, Phys. Rev. 127, 545 (1962).

just beyond the exit of the beam analyzing magnet. Counting was stopped during beam on time by electronically grounding one coincidence circuit output. A block diagram of the electronics used is shown in Fig. 2. While studying the  $B^{12}$  decay the beam was on target for 1 msec, and deflected off target for 35 msec. Counting duration was 25 msec, starting 4 msec after the beam was deflected. For the  $N^{12}$  measurement, bombardment lasted 18 msec, with the beam off 25 msec. Counting started 5 msec after beam deflection and continued for 17 msec. The differences in the two cycles are due to the different half-lives of the activities studied, and the difference in cross sections of the two reactions at the bombarding energies used.

The target chamber and detector positions are shown in Fig. 3. The beta particles were counted in coincidence by a two-stage detector using plastic fluors as scintillators. The axis of this detector was at  $45^\circ$  to the beam direction. A graphite collimator defined the beta particle detector solid angle ( $\sim 1\%$  of  $4\pi$ ). Just behind the collimator was a 2.5-in.  $\times$  2.5-in.  $\times$  3/32-in. plastic fluor, whose short axis was parallel to the axis of the collimator. This fluor was viewed from two opposing ends through 1-in.-long Lucite light pipes by 6292 DuMont photomultipliers. The two tubes selected were quite close in sensitivity, and had good signal-to-noise ratios. More precise gain equalization was achieved by using two high-voltage supplies, and setting their voltages to equalize output pulse heights from each tube, using a  $Cs^{137}$  source to generate pulses. The signal outputs from these two photomultipliers were paralleled using short lengths of RG-71/U cable, and put into a single pre-amplifier and amplifier. This arrangement gave reasonably uniform pulse heights out for beta particles passing through all regions of the fluor.

Immediately behind this fluor was a right cylindrical fluor 4-in. diam and 2 in. high, viewed end on by a DuMont 6364 photomultiplier. A thin paper light baffle between fluors prevented the light originating in either fluor from scattering into the other. A coincidence between the signals from each detector section was required to give a beta-particle count. The output pulses from the larger fluor were displayed on the 100-channel analyzer frequently, with the analyzer gated by the beta coincidences, to check that the proper beta spectrum was being measured. A typical  $B^{12}$  beta spectrum obtained with the large fluor is shown in Fig. 4, along with the beta spectrum of a  $Ce^{144}$ - $Pr^{144}$  source which was used to give a 2.98-MeV energy calibration point. A sample  $N^{12}$  spectrum is shown in Fig. 5.

Gating times were varied as a check on possible longer lived backgrounds present. In the case of  $B^{12}$ , with a beam on target time of 1.5 msec, and time per cycle of 150 msec, the beta counter was gated on for 20 msec at 10, 60, and 120 msec after beam off time. The relative counting rates were in good agreement with the half-life of  $B^{12}$ ,<sup>1</sup> indicating that any longer lived activities were not present in sufficient quantities to be a problem.

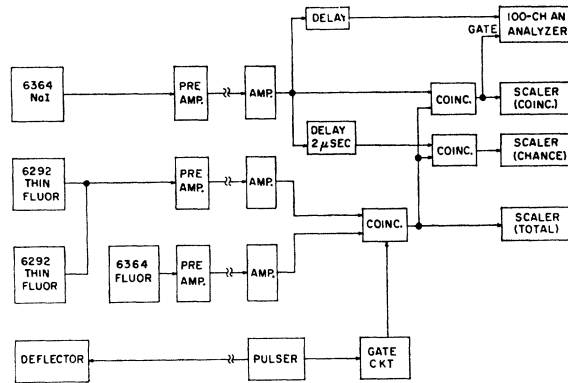


FIG. 2. Block diagram of electronics used in the  $B^{12}$  and  $N^{12}$  branching ratio measurements.

Similar delayed counting was done with  $N^{12}$ , with the same negative results. Background due to the beam itself was measured by placing a piece of 5-mil gold in the target position and counting in the usual way. This background was found to be negligible. The accidental beta particle counting rate was monitored occasionally by placing a 2- $\mu$ sec delay in one signal line to the coincidence unit, and was never greater than 0.3% of the true counting rate.

Taking into account the bias of the beta counter, and the mean energy loss of the beta particles in passing through the target, target backing, and thin fluor, it was calculated that only those beta particles emitted in

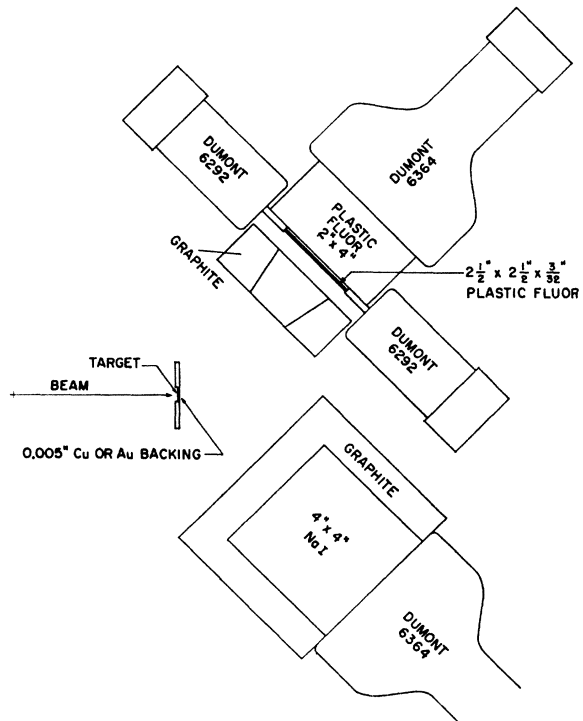


FIG. 3. Diagram of target and detector positions for the  $B^{12}$  and  $N^{12}$  branching ratio measurements.

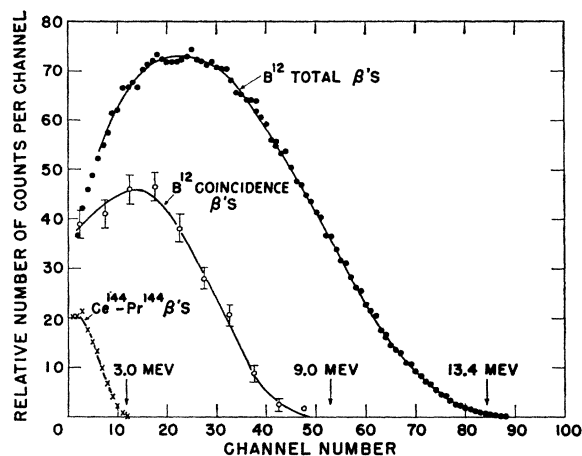


FIG. 4. Pulse-height distributions of total  $B^{12}$  beta decay, of  $B^{12}$  beta decay counted in coincidence with the 4.43-MeV gamma rays of  $C^{12}$ , and of the  $Ce^{144}$ - $Pr^{144}$  beta decay, all measured with the 4-in.  $\times$  2-in. fluor.

the target with energies equal to or greater than 2.1 MeV were counted. Since this effective threshold eliminated a greater fraction of the beta spectrum to the 4.43-MeV level than to the ground state, a correction factor of 1.090 was applied to the  $B^{12}$  measurement, and a factor of 1.034 to the  $N^{12}$ .

At  $45^\circ$  to the beam and  $90^\circ$  to the axis of the beta particle detector (Fig. 3) was the gamma-ray detector consisting of a 4-in.  $\times$  4-in. NaI(Tl) crystal mounted on a DuMont 6364 photomultiplier tube. A 1.5-in.-thick graphite cup was placed over the NaI crystal to reduce background. The 4.43-MeV  $C^{12}$  gamma rays were counted in coincidence with the beta particles to give the number of decays to the 4.43-MeV level, as shown in Fig. 2. The standard Los Alamos coincidence units used in this experiment had adjustable delays on each input which were set experimentally by maximizing the coincidence rate. These delays took care of time differences in signal arrival times due to differences in transit times through the electronics used, and also to the difference in scintillator response times.

The branching ratio is given by the expression

$$\rho = 4\pi f N_\gamma / \epsilon_\gamma \Omega_\gamma N_\beta,$$

where  $f$  is the beta particle bias correction factor discussed above,  $N_\gamma$  is the 4.43-MeV gamma-ray coincidence counting rate,  $\epsilon_\gamma$  is the efficiency and  $\Omega_\gamma$  the solid angle in steradians of the gamma-ray detector, and  $N_\beta$  is the total beta particle counting rate.

In order to determine the product of the efficiency and solid angle ( $\epsilon_\gamma \Omega_\gamma$ ) of the gamma-ray detector for 4.43-MeV gamma rays, a Po-Be source, which could be placed at the target position, was calibrated in terms of the total number of 4.43-MeV gamma rays emitted per sec. This was done by first measuring the counting rate with the Po-Be source at several distances from the 4-in.  $\times$  4-in. NaI crystal photomultiplier combination. This

procedure was then repeated using 3-in.  $\times$  3-in. and 2-in.  $\times$  1-in. NaI crystals. The resulting Po-Be gamma-ray spectrum measured with the 4-in.  $\times$  4-in. NaI crystal is shown in Fig. 6. Since considerable background is present in the Po-Be spectrum at lower energies, the  $N^{15}(p,\alpha\gamma)C^{12}$  reaction, which produces the 4.43-MeV gamma ray with relatively low background, was utilized to determine that part of the lower energy Po-Be spectrum due to the 4.43-MeV gamma rays. A  $N^{15}$  gas target was bombarded with 3-MeV protons, and the 4.43-MeV gamma rays produced in this manner counted with all three crystals. A pulse-height distribution taken with the 4-in.  $\times$  4-in. NaI crystal is shown in Fig. 6, and the low-energy end shows a noticeable improvement in background over the Po-Be spectrum. Using the high-energy end of the Po-Be spectrum, and the shape of the low-energy end of the  $N^{15}(p,\alpha\gamma)C^{12}$  spectrum, the number of counts due to 4.43-MeV gamma rays from the Po-Be source was calculated. A Los Alamos IBM 704 code, which took into account crystal dimensions, source distance, and source dimensions, was used to obtain the crystal efficiencies from which the source strength was calculated. The source calibrations obtained with the three crystals all agreed to better than 1.5%, and gave an average value of  $2.04 \times 10^4$  gamma rays per sec at the time of the calibration. This value was corrected for the decay of the  $Po^{210}$  ( $T_{1/2} = 138.4$  days) whenever the Po-Be source was used to calibrate the gamma-ray detector.

With the Po-Be source calibrated, a series of runs was made to measure the two desired branching ratios. Data were taken alternately on the  $N^{12}$  and  $B^{12}$  decays until enough counts were obtained on each to give better than 3% statistics. Before and after each branching ratio run, the Po-Be source was placed at the target position, and the gamma-ray pulse-height distribution measured, after which the background counting rate of

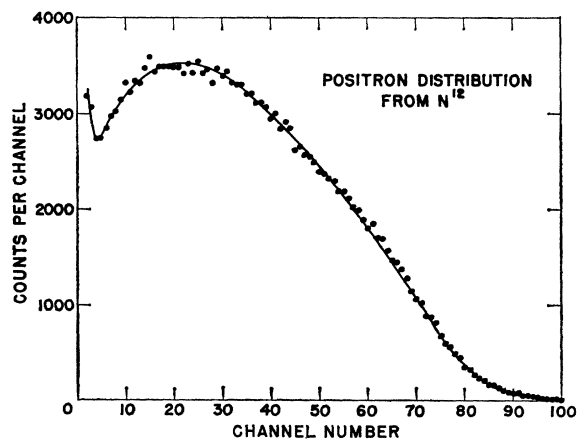


FIG. 5. Pulse-height distribution of total  $N^{12}$  positron decay taken with the 4-in.  $\times$  2-in. fluor. The 3- $\mu$ sec gate width of the 100-channel analyzer accounts for most of the low-energy background shown. The shorter resolving time of the coincidence unit reduced this background on the scaler counts to a negligible amount.

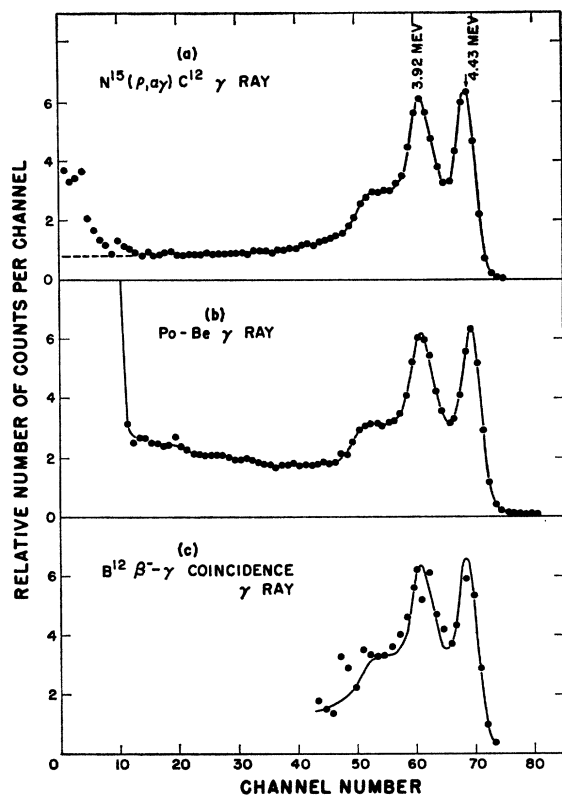


FIG. 6. (a) Pulse-height distribution of 4.43-MeV gamma rays from the  $N^{15}(\beta, \alpha\gamma)C^{12}$  reaction. (b) Pulse-height distribution of 4.43-MeV gamma rays from the Po-Be source. (c) Pulse-height distribution of 4.43-MeV gamma rays from the  $B^{12}$  decay counted in coincidence with the emitted beta particles.

the gamma-ray detector with the source out was determined. From these measurements the value of  $\epsilon_\gamma\Omega_\gamma$  was calculated. This calibration gave a value on the order of 0.34 sr for the product  $\epsilon_\gamma\Omega_\gamma$ . Due to small variations in the threshold voltage of the gamma-ray detector, this number changed slightly from run to run. The threshold voltage for counting gamma rays was left at the same nominal value for all gamma-ray counting, at a point which was just below the peaks of the 4.43-MeV gamma-ray pulse-height distribution. Since this portion of the spectrum is relatively flat, counting rates were quite insensitive to small changes in the threshold voltage. With the gamma-ray counting threshold set at this level, most of the lower energy background was excluded, helping to minimize the accidental counting rate. The accidental counting rate was measured on each run by sending the beta-particle and gamma-ray signals into a coincidence unit with 2  $\mu$ sec of delay in the gamma-ray signal line (Fig. 2), and recording the coincidence output on a scalar. The biases of the two counting systems were matched by using a  $Co^{60}$  gamma-ray source at a distance of 50 ft from the detector as a random source, and adjusting the biases until the counting rates were equal. Accidental rates were kept on the order of one-half the true counting rate or less

by adjusting the beam current. In addition to accidentals, a small background attributable to cosmic-ray events was observed with the beam off. These were true coincidences, and had to be subtracted from the coincidence totals.

The 4.43-MeV reaction gamma rays were displayed on the 100-channel analyzer with the analyzer gated by the  $\beta\gamma$  coincidences. A delay was inserted in the gamma-ray signal line to the analyzer to match the delay in the coincidence unit. A typical  $B^{12}$  4.43-MeV gamma-ray spectrum obtained in this manner is shown in Fig. 6.

With the 100-channel analyzer gated by the  $\beta\gamma$  coincidences, the beta-particle detector output was displayed on the 100-channel analyzer during a  $B^{12}$  run. This should record the beta-particle spectrum to the 4.43-MeV  $C^{12}$  level, and the observed spectrum is shown in Fig. 4. The end-point energy of this spectrum is  $\sim 4.4$  MeV below the end point of the total beta spectrum, verifying that the coincidences being measured are those resulting from decays to the 4.43-MeV level of  $C^{12}$ .

## Results

The branching ratios to the 4.43-MeV level of  $C^{12}$  measured in this experiment were  $(1.3 \pm 0.1)\%$  for  $B^{12}$ , and  $(2.4 \pm 0.2)\%$  for  $N^{12}$ . The ratio of the  $N^{12}$  to the  $B^{12}$  branching ratio is  $1.84 \pm 0.1$ .

The ratio of  $N^{12}$  to  $B^{12}$   $ft$  values for transitions to the 4.43-MeV level of  $C^{12}$  was calculated to be  $0.92 \pm 0.06$ . The half-lives measured in Part II of this paper were used in this calculation.

## PART II

### $B^{12}$ and $N^{12}$ Half-life Measurements

Using published values of half-lives and end-point energies available in January, 1961, the ratio of  $ft$  values of the  $N^{12}$  to  $B^{12}$  transitions to the ground state of  $C^{12}$  was calculated to be  $1.22 \pm 0.04$ .<sup>7</sup> The half-lives used in this calculation were that of Schardt<sup>8</sup> for  $B^{12}$  ( $20.31 \pm 0.20$  msec), and that of Vedder<sup>2</sup> for  $N^{12}$  ( $11.43 \pm 0.05\%$ ). Since this large difference of the ratio of  $ft$  values from unity was unexpected in view of the usual assumption of charge symmetry, a measurement of the  $B^{12}$  and  $N^{12}$  half-lives was carried out to see whether any part of the discrepancy could be found in the half-life values. A single experiment to measure the two half-lives has the advantage that their ratio is somewhat more accurate than the measured half-lives themselves due to the partial cancellation of systematic errors, and it is the ratio of half-lives which is used in the calculation.

The  $N^{12}$  activity was produced by bombarding a thick boron target, enriched to 96%  $B^{10}$ , with 5.25-MeV  $He^3$  particles accelerated by the large Los Alamos Van de

<sup>7</sup> N. W. Glass, R. W. Peterson, and R. K. Smith, Bull. Am. Phys. Soc. **6**, 49 (1961).

<sup>8</sup> A. W. Schardt, Phys. Rev. **122**, 1871 (1961).

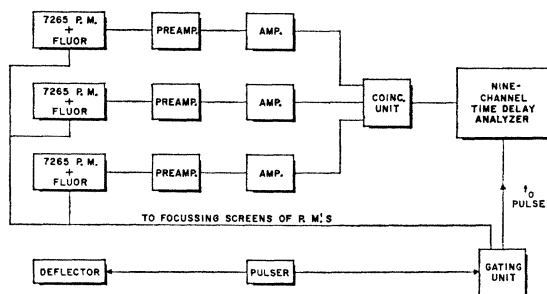


FIG. 7. Block diagram of the electronics used in the  $B^{12}$  and  $N^{12}$  half-life measurements.

Graaff.  $B^{12}$  was produced by bombarding the same target with 2-MeV deuterons. The  $B^{11}(d,p)B^{12}$  cross section was sufficiently large that it was not necessary to change to a normal boron target to produce  $B^{12}$ .

The beta particles were bent by a uniform field beta-ray spectrometer onto an exit slit defined by three small plastic fluors placed one behind the other, each viewed through quartz light pipes by a 7265 RCA photomultiplier tube. By requiring a coincidence between the signals from the three fluors to give a beta-particle count, background was kept to a minimum. This spectrometer was constructed for the purpose of comparing the shapes of the  $B^{12}$  and  $N^{12}$  ground-state spectra as a test of the conserved vector current theory, and is described in detail in another paper.<sup>5</sup> The spectrometer had five similar exit channels at different radii, of which only the center channel was used in this experiment, and the spectrometer field was set so that the peak of the beta spectrum being observed was centered in the center channel. The field of the spectrometer was regulated by feeding back an error signal from a nuclear magnetic resonance gaussmeter to the magnet power supply. A block diagram of the electronics is shown in Fig. 7.

The bombarding particles were gated by electrostatic deflection. Counting gating was accomplished by pulsing the voltage on the focusing screens of the photomultiplier tubes. After the beam had been swept off target, the gating unit put out to a  $t_0$  pulse starting a nine-channel time-delay analyzer, which then counted pulses occurring in time between  $t_0$  and  $t_0 + 9\Delta t$ , in nine equal time-channel lengths of  $\Delta t$ . This analyzer was designed by Glore, and has been described previously.<sup>9</sup> The channel lengths were calibrated with a 100-kc/sec crystal oscillator, and were found to be equal to better than  $\pm 0.5\%$ .

$N^{12}$  data were taken with channel lengths of 5, 10, and 15 msec, and  $B^{12}$  data with channel lengths of 5, 10, 20, and 30 msec. The longer channel length data showed that background was not a serious problem. Accidentals were checked by inserting 2  $\mu$ sec of delay in each of the three signal lines separately, and found to be small enough to ignore.

<sup>9</sup> J. P. Glore, Los Alamos Scientific Laboratory Report LA-2152, 1958 (unpublished).

## Results and Discussion

The  $N^{12}$  data are shown in Fig. 8, normalized for convenient plotting, and statistical errors are indicated wherever appreciable. The three slopes agreed within experimental error, and a weighted least-squares fit of the data gave a value of  $11.0 \pm 0.1$  msec for the half-life of  $N^{12}$ , somewhat shorter than previous values.<sup>1,10</sup> The least-squares fit of the  $B^{12}$  data, shown in Fig. 9, gave a value of  $20.2 \pm 0.2$  msec for the half-life of  $B^{12}$ . This measured half-life is in good agreement with previous values.<sup>1,8</sup>

Using these measured half-lives, the ratio of  $ft$  values of the  $N^{12}$  to  $B^{12}$  ground-state transitions was calculated, taking<sup>11</sup>  $13.369 \pm 0.001$  and<sup>12</sup>  $16.43 \pm 0.06$  MeV as the maximum energies of the  $B^{12}$  and  $N^{12}$  spectra, respectively. An independent check on the ratio of these end-point energies was obtained while carrying out the comparison of the ground-state spectra mentioned above,<sup>5</sup> which was in agreement with the ratio calculated using the above end-point energies. The percentages of  $B^{12}$  and  $N^{12}$  decays to the ground state of  $C^{12}$  were found by subtracting the known branching fractions to excited levels in  $C^{12}$ , which are listed in Table I. Branching fractions to the 4.43-MeV level of  $C^{12}$  are those measured in Part I of this paper. The  $N^{12}$  branch to the 10.1-MeV

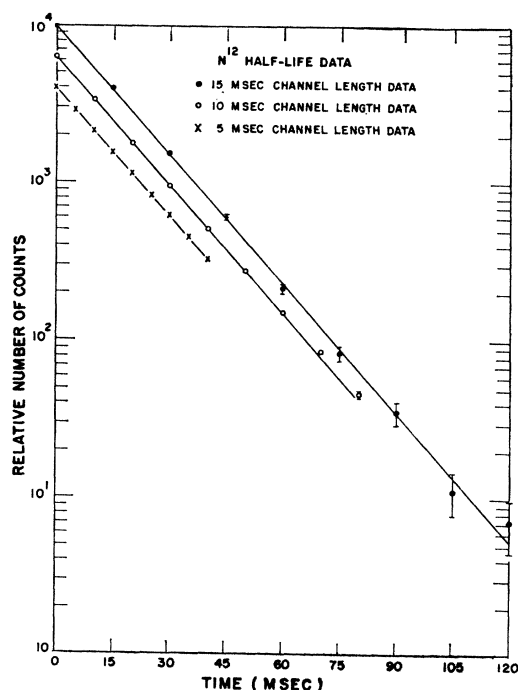


FIG. 8.  $N^{12}$  half-life data. The ordinate scale is in arbitrary units.

<sup>10</sup> B. J. Farmer and C. M. Class, Bull. Am. Phys. Soc. 4, 278 (1959).

<sup>11</sup> F. Everling, L. A. König, and J. H. E. Mattauch, Nucl. Phys. 15, 342 (1960).

<sup>12</sup> F. Ajzenberg-Selove, M. L. Bullock, and E. Almqvist, Phys. Rev. 108, 1284 (1957).

TABLE I. Branching fractions of  $B^{12}$  and  $N^{12}$  to levels of  $C^{12}$ .

$E_x(C^{12})$ (MeV)	$B^{12}$ branching fraction (%)	$N^{12}$ branching fraction (%)
0	97.3	93.5
4.43	$1.3 \pm 0.1$	$2.4 \pm 0.2$
7.66	$1.3 \pm 0.4^a$	$3.0 \pm 0.5^b$
10.1	$0.13 \pm 0.04^a$	$(1.1 \pm 1.1)^c$

<sup>a</sup> See reference 14.

<sup>b</sup> See reference 6.

<sup>c</sup> Estimated from the measured  $B^{12}$  branch to the 10.1-MeV level by assuming the equality of  $ft$  values of transitions to the same level.

level of  $C^{12}$  was obtained by assuming equality of its  $ft$  value with the  $ft$  value of the  $B^{12}$  transition to the same level. The ratio of  $f$  values was found by numerical integration of tables published by the National Bureau of Standards.<sup>13</sup> This procedure gave  $1.16 \pm 0.03$  as the ratio of the  $N^{12}$  ground-state transition  $ft$  value to the  $B^{12}$  ground-state transition  $ft$  value.

In view of this difference in  $ft$  values of the ground-state transitions, the method of obtaining the  $N^{12}$  branching ratio to the 10.1-MeV level of  $C^{12}$  is questionable. However, the ratio of  $ft$  values of the ground-state transitions is not particularly sensitive to this number. In order to estimate the error of the calculated ratio of ground-state  $ft$  values, an error for the  $N^{12}$  10.1-MeV branch equal to the branch itself, was assumed. The calculated error of the ratio of  $ft$  values thus includes the possibility of no  $N^{12}$  decays to the 10.1-MeV level of

$C^{12}$ , which possibility would bring the ground-state  $ft$  values nearest to equality.

Not included in the estimated error is the possible existence of other beta transitions to higher levels of  $C^{12}$ . However, it is probable that such decays would tend to make the ratio of ground-state  $ft$  values even larger due to the greater amount of energy available to the  $N^{12}$  decays than to the  $B^{12}$  decays.

Thus, in view of the accuracy with which the necessary quantities for calculation of the  $ft$  values of the ground-state transitions are known, it appears that there is a real difference in the  $B^{12}$  and  $N^{12}$  ground-state transition  $ft$  values.

### PART III

#### $B^{10}(He^3, n) N^{12}$ Cross-Section Measurement

Before performing an experimental comparison of the shapes of the  $B^{12}$  and  $N^{12}$  ground-state spectra,<sup>5</sup> it was necessary to determine whether or not there would be a significant shift in the  $B^{12}$  and  $N^{12}$  source positions, formed by bombarding a thick, enriched boron target with  $He^3$  particles and deuterons, due to possible differences in the shapes of the thin target excitation curves of the  $B^{11}(d, p)B^{12}$  and  $B^{10}(He^3, n)N^{12}$  reactions. For this reason the thin-target cross section for the  $B^{10}(He^3, n)N^{12}$  reaction was measured as a function of bombarding energy over the energy range 2.0 to 6.3 MeV. Previously, a thin target cross section had been measured at 2.54 MeV.<sup>12</sup> The thin target excitation curve for the  $B^{11}(d, p)B^{12}$  reaction was already established over the desired range.<sup>3</sup>

The apparatus used was that employed in the branching ratio measurements described in Part I of this paper, with only the beta-particle detector being used. A thin target of boron enriched to 96%  $B^{10}$  was deposited on a 1-mil gold backing by evaporation from a tungsten filament in vacuum. The gold foil was masked off to give a circular target 1-cm diam. Target thickness was measured by weighing the foil before and after evaporation. The target was placed in the target holder on the 5-mil brass exit window (Fig. 3), and bombarded with  $He^3$  particles. After passing through the  $90^\circ$  analyzing magnet, the beam was gated by electrostatic deflection. The beam was on target for 12 msec, and off for 20 msec. Counting duration was 13.5 msec, starting 2.5 msec after the beam was swept off target. The positrons were counted in coincidence by the two-stage beta-particle detector (Fig. 3), and the positron spectrum displayed on the 100-channel analyzer. Counting thresholds were set somewhat higher than in the branching ratio measurements, permitting the use of larger beam currents with no appreciable increase in the accidental rate. With constant voltage thresholds and gating times, the number of positrons counted at each bombarding energy was directly proportional to the number of  $N^{12}$  nuclei formed. Thus, a relative thin target cross section curve was determined by bombarding the target with equal

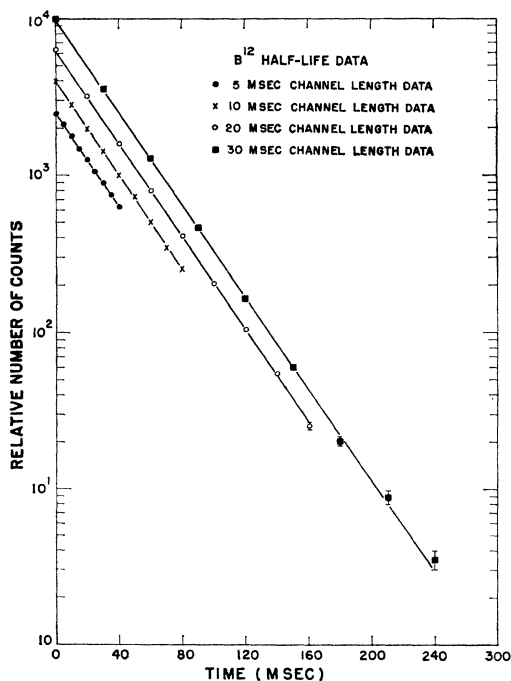


FIG. 9.  $B^{12}$  half-life data. The ordinate scale is in arbitrary units.

<sup>13</sup> Tables for the Analysis of Beta Spectra, National Bureau of Standards, Applied Mathematics Series 13 (1952).

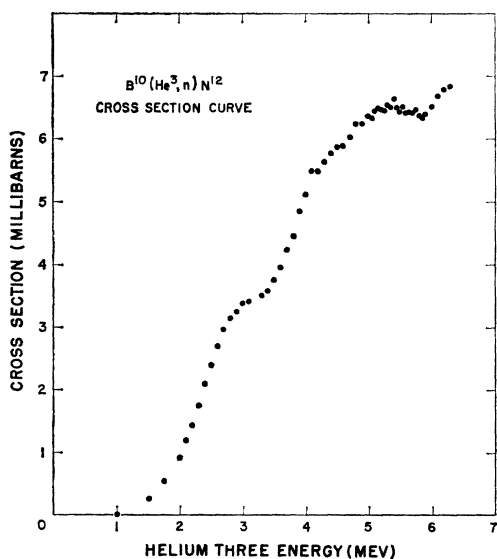


FIG. 10.  $B^{10}(\text{He}^3, n)\text{N}^{12}$  cross-section curve.

numbers of  $\text{He}^3$  particles at each desired energy, and plotting the number of positrons counted at each bombarding energy vs the bombarding energy. The amount of charge delivered to the target was measured to better than 1% by a current integrator.

Although only the relative cross section curve was essential to the experimental comparison of the  $B^{12}$  and  $N^{12}$  ground-state spectra,<sup>5</sup> the measured curve was normalized to absolute cross sections, as very little cross-section data on the  $B^{10}(\text{He}^3, n)\text{N}^{12}$  reaction are available. To normalize the cross-section curve, the thick target yield was measured at several energies in the 2.0 to 6.3 MeV energy range, and these yields then corrected for absorption and bias, gating, and solid angle of the beta-particle detector. The thin-target relative cross-section curve was integrated between each consecutive pair of thick-target bombarding energies,

and equated to the differences of the measured thick-target yields. This procedure gave several values of the normalization constant which were in good agreement with one another, and also determined the thickness of the  $B^{10}$  in the thin target to be 70 keV for 2-MeV  $\text{He}^3$  particles. This target thickness was in agreement with the less accurate value determined by weighing.

As a check on the experimental procedure, a thick, normal boron target was bombarded with deuterons at several energies in the 1.5- to 3.0-MeV energy range, and the thick target yield calculated at each bombarding energy from the measured beta particle counts. The thin-target  $B^{11}(d, p)B^{12}$  cross-section curve of Kavanagh and Barnes,<sup>3</sup> normalized at 1.65 MeV to the value of Cook *et al.*,<sup>14</sup> was then integrated between each consecutive pair of bombarding energies to give another set of values for the yields. The two groups of yields were in good agreement.

The  $B^{10}(\text{He}^3, n)\text{N}^{12}$  thin-target cross-section curve measured in this experiment is shown in Fig. 10. The point size is equal to or greater than the statistical error in the number of counts taken at each point. The error in the absolute value of the cross sections is  $\pm 30\%$ . From Fig. 10, the cross section at 2.54 MeV is  $2.5 \pm 0.8$  mb, to be compared with the value of  $5.2_{-1.6}^{+2.1}$  mb of Ajzenberg-Selove *et al.*<sup>13</sup> It is seen that there is some disagreement between the two values.

#### ACKNOWLEDGMENTS

The authors wish to express their thanks to J. L. McKibben and the members of the accelerator group for many hours of machine time and frequent helpful discussions. Particular thanks are due R. K. Smith of this group for his active assistance with the branching ratio measurements, and to W. M. Visscher of the theoretical division for stimulating discussions of the ground state *ft*-values discrepancy.

<sup>14</sup> C. W. Cook, W. A. Fowler, C. C. Lauritsen, and T. Lauritsen, *Phys. Rev.* **111**, 567 (1958).